Comportamiento de los agregados de Bogotá ante cargas cíclicas
Cyclic behavior of Bogotá unbound aggregates

B. Caicedo
Universidad de los Andes, Bogotá Colombia

O. Coronado
Universidad de la Salle, Bogotá, Colombia

J.M. Fleureau
Ecole Centrale Paris & CNRS, Châtenay Malabry, France

A.Gomes Correia
Universidade do Minho, Guimarães, Portugal

RESUMEN

En este artículo se presentan los resultados de un trabajo experimental sobre tres diferentes materiales granulares de la Sabana de Bogotá. El trabajo experimental incluye ensayos triaxiales con cargas cíclicas y con medida de la presión intersticial negativa (succión). Sobre los tres materiales se estudió la influencia de diferentes parámetros tales como la densidad, la humedad y el contenido de finos. La interpretación de los resultados en el dominio de deformaciones quiasi-elástico se hace tanto en términos de esfuerzos totales como de esfuerzos efectivos lo cual permite tener en cuenta la influencia de la presión intersticial negativa con la perspectiva de utilizarlos en diseños de pavimentos más racionales.

ABSTRACT

The results of an experimental work on three road granular materials from La Sabana de Bogotá are presented. These works include small strains precision triaxial tests under cyclic loading with measurement of the negative pore water pressure (suction). The influence of different initial conditions of density, water content and fines content was studied. The interpretation of the results, in the quasi-elastic domain, is based on total stress and effective stress analyses , the latter allowing to take into account the effects of both total stresses and negative pressure, in the perspective of a more rational design of pavement layers.

Keywords: Roads, unsaturated unbound materials, modulus

1 INTRODUCTION

The empirical nature of traditional pavement design methods has been discussed in road engineering for many years. These methods rely on empirical rules based on experience under particular conditions. The main limitation of empirical methods is that they cannot be extrapolated with confidence beyond those conditions on which they are based (Lekarp et al. 2000).

On the other hand, mechanistic pavement design is based on rational methods using Young' modulus (E) and Poisson's ratio (ν). A conditional prerequisite for the success of the mechanistic approach is that the behavior of the constituent materials is properly understood. Numerous research has been conducted on the behavior of unbound granular materials (U.G.M.) used in flexible pavements. Most of these works has been carried out on good quality granular materials whose index properties are based on the recommendations of empirical methods.

Non standard granular materials could have characteristics like higher fines content, higher plasticity index, higher blue methylene value and more crushable grains than good quality U.G.M. Most of these characteristics increase the role of the water on the mechanical behaviour of U.G.M. For this reason, to analyze the role of index parameters on the performance of flexible pavements it is essential to take in to account the influence of negative pore pressure on the Young' modulus (E) and Poisson's ratio (ν).

In the laboratory, the negative pore water pressure, or suction ($u_c = u_a - u_w$), is not easy to measure in coarse materials and their derivation requires the use of elaborate tests.

Several authors have studied the effect of the negative pore water pressure on the small strains behavior of partially saturated soils (Brull 1980, Wu et al. 1989, Kheirbek-Saoud 1994, Picornell and Nazarian 1998, Balay et al. 1998). In most cases, the analysis of the results is made in total stresses, and the role of the stress tensor is considered separately from that of the negative pore water pressure. Other

authors (Wu et al. 1989, Biarez et al. 1991, Coussy & Dangla 2002, Fleureau et al. 2003) showed that an effective stress approach could be used to take in account the effect of the capillary pressure in the interpretation of the data in the very small strains domain.

In this study, small strains triaxial tests with measurement of negative pore water pressure have been performed on three "non standard" unbound granular materials (U.G.M.) used in Bogotá Colombia. The Colombian materials have recomposed in order to attain different plasticity index, methylene blue value, crushability and fines content. Wetting tests have been carried out to determine suction and water content changes in the material during wetting. One of the goals of this paper is to show how to take moisture changes into account in the pavement design analysis using an effective stress approach.

2 MATERIALS AND METHODS

2.1 *Materials*

The materials used in this study are gravels made of sandstones coming from three different locations near Bogotá - Colombia. The three gravels (Servitá, Vista Hermosa and Soacha) have different degrees of cementation that affects their state properties. Also two alluvial sands were used in order to prepare mixtures with controlled characteristics. The state properties of the five materials are summarized in Table 1.

Table 1: Main state properties of the materials

	Plasticity Index %	Blue Methylene (g/100g)	Abrassion coeff. Los Angeles %
Vista Hermosa	9	1.40	20
Servitá	10	1.46	34
Soacha	16	1.90	56
Guamo sand	--	0.90	--
Suarez sand	--	0.50	--

Using these five basic materials, a total of 25 different mixtures were prepared. These mixtures have different fine contents, plasticity indexes, blue methylene, fragmentability and water content values.

2.2 *Cyclic triaxial tests*

The cyclic tests were carried out in a classic triaxial cell, allowing a direct measurement of the stiffness modulus and Poisson's ratio for homogeneous strains ranging between 10^{-6} and 10^{-2}. To be able to explore the domain of the very small strains with sufficient accuracy, the force and strain measurements are done on the specimen itself. The force transducer is placed inside the cell directly on the head of the specimen, which permits a precise measurement of the force applied to the specimen and eliminates the bearing-piston friction problems. The measure of the axial strains is achieved by means of three LDT strain sensors placed in the central zone of the specimen, in order to avoid the influence of the constrictions of the bases on the measures. Radial strains are derived from the variations of the perimeter of the specimen measured by a deformable belt placed to mid-height and equipped with a LDT sensor. The LDT sensors are constituted of 4 strain gauges forming a complete Wheatstone bridge fixed on a deformable blade made of beryllium bronze; they were manufactured at the Ecole Centrale Paris on the model of the sensors developed at the university of Tokyo in the team of Professor Tatsuoka (Goto et al. 1991). Supports for the sensors are put in place in the specimen during the compaction. The accuracy of the strain measurements is approximately10^{-5} with a 21 bits Agilent A/D converter. To prepare the specimens, water is added to the dry mixture in a homogenous way. Dynamic compaction of the specimen, 150 mm in diameter and 300 mm in height, is achieved by hand by means of a Modified Proctor hammer, in 12 layers with 56 strokes of rammer per layer. During the manufacture of the specimens, special attention is paid to the setting up of the six supports of the vertical sensors. Then, the axial and radial strain sensors are put in place, as well as the force transducer.

Figure 1: Triaxial sample with vertical and radial LDT transducers

To determine the reversible behavior of the materials, preliminary conditioning of the specimens is carried out in order to simulate the real conditions of laying down of the soil: it consists in 20000 loading-unloading cycles under an isotropic stress of 40 kPa and a deviatoric stress of 280 kPa. After the pre-conditioning, the specimen is submitted to 20 successive paths with increasing levels of stress (Figure 2a). All the tests are made under constant confining stress σ_3.

Each loading is applied during 100 cycles. The reversible strains of the specimen are measured during the 100th cycle. An example of the measurements is shown on Figure 2b, where the deviatoric stress q is represented versus the axial, radial and volumetric strains (ε_1, ε_3 and ε_v, respectively).

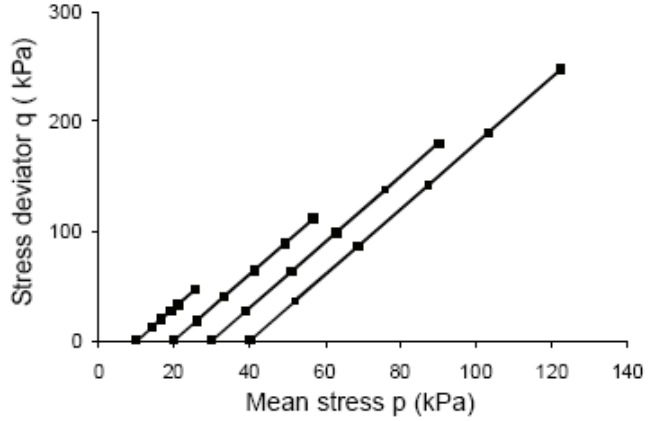

Figure 2a: Stress paths for the determination of the elastic properties of the materials.

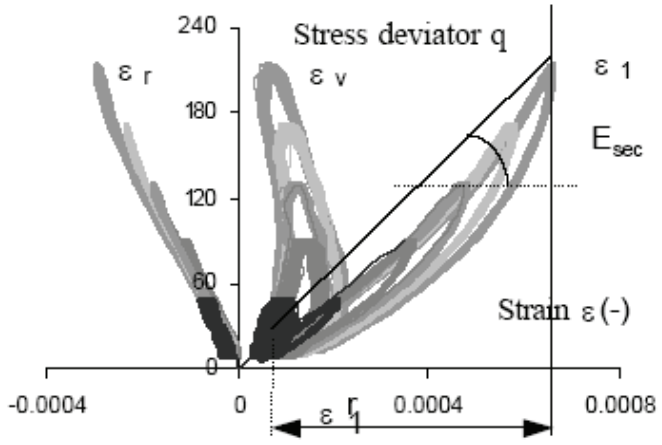

Figure 2b: Example of measurement of the stress deviator vs. axial, radial and volumetric strains.

These cycles illustrate the non linearity of the behavior, i.e. the increase in the modulus with q, when the axial strain exceeds the elastic limit of the material (about10^{-5}).

The secant module is defined in the following way:

$$E_{sec} = q / \varepsilon_1^r \qquad (1)$$

The measurements are made for axial strain ε_1^r approximately equal to 10^{-4}.

2.3 *Triaxial tests with measurement of the negative pore water pressure*

The device consists of a triaxial cell with a semi-permeable ceramics placed in the base; the porous stone with high air entry pressure (1,5 MPa, from Soil Moisture) does not permit the passage of air in the water circuit. The device can be used either as a tensiometer (with $u_a = 0$ and $u_w < 0$) to measure negative pore water pressures between 0 and 50 kPa, or with an air overpressure at the head of the specimen for higher negative pressures. Pore water pressure measurements are done by means of an absolute pressure sensor with a range of 1000 kPa and a sensitivity of 0,1 kPa/mV. Data logging is achieved by means of a 16 bits data acquisition system from GDS.

The size of the specimens is 100 mm in diameter and 200 mm in height.

Specimens were dynamically compacted by means of a Modified Proctor hammer in 4 layers, with 56 strokes per layer. A thin layer of kaolinite is placed on the ceramics to ensure a good contact with the specimen and the continuity of the water phase.

2.4 *Wetting tests on tensiometric plates*

To impose negative pore water pressures ranging between 0 and 30 kPa, tensiometric plates were used. They are made of a a low porosity sintered glass filter, that plays the role of the semipermeable separation, set in a glass funnel. The specimen is placed on the filter to the atmospheric pressure, in contact with a reservoir filled with de-aired water. Imposing a difference of level between the filter and the measurement tube results in controlling the depression of the water placed in the reservoir, and therefore the negative pore water pressure in the specimen.

At the end the cyclic triaxial tests, the specimen is cut into several pieces, that are placed on the tensiometric plate. The exchanges of water between the specimen and the reservoir are derived from the displacement of the water meniscus in a horizontal measurement tube connected to the reservoir. When the negative pore water pressure in the specimen reaches the imposed value, generally at the end of 5 days, the total volume of the specimen and its water content are derived from immersion in kerdane followed by drying in an oven; the water content, void ratio and degree of saturation of the material are derived from these data.

3 INTERPRETATION OF THE RESULTS IN TOTAL STRESS, ROLE OF THE PLASTICITY INDEX AND FINES CONTENT

Two sets of tests were performed on materials having 10% of fines: one set corresponds to a plasticity index of 16% (IP=16%) and the other to an IP=0. Figures 3 and 4 illustrate the variation of the secant modulus with the isotropic stress p in two planes (logp – log E_{sec}) and (p – E_{sec}) for different water contents ranging from 3.0% to 5.8%. One notes the sensitivity of the material to this

parameter: under the same isotropic stress, the modulus is higher when the water content is smaller because of the increase in the capillary forces in the menisci that form themselves between the grains.
As previously noted (Fleureau et al. 2003), the lines are more or less parallel for the different wet soils; this is particularly clear on the logarithmic plan.

The logarithmic plan allows the use of exponential models like the K-θ model. On the other hand, the results on the linear plan adjust to straight lines having different slope depending on the plasticity index. This kind of plan allows the normalization of the results using the modulus E_{0p} corresponding to zero total mean stress (p=0).

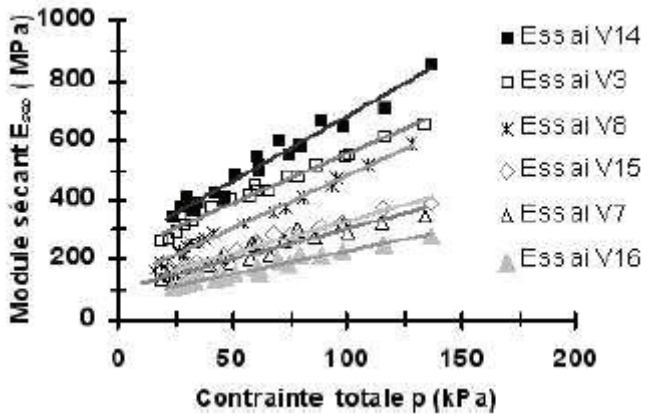

Figure 3: Results for zero plasticity index (bleu value = 0.5g/100g), logarithmic scale.

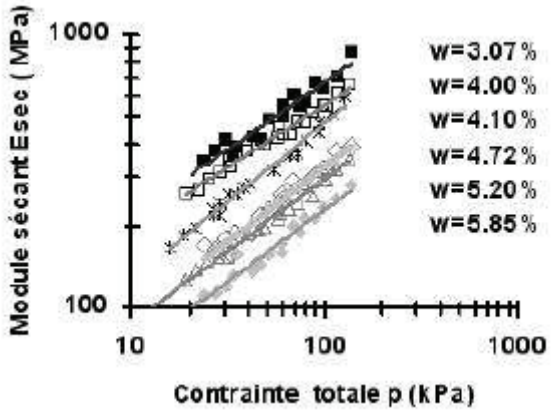

Figure 4: Results for zero plasticity index (bleu value = 0.5g/100g), linear scale.

The linear interpretation allows the normalisation of the results dividing by the modulus E_{0p} (figure 5). This figure shows that all the points for the same plasticity index are grouped along the same line. We remark that the higher the plasticity index, the smaller the slope of the line. Equations 2 and 3 describe the variation of the secant modulus for 0% and 16% plasticity index and for 10% of fine content.

It's well known that the modulus increases as the water content reduces (Balay et al., 1998; Fleureau, et al., 2002). This is particularly clear for the modulus at zero total mean stress (E_{op}). Furthermore, since water content and suction are directly related, the modulus E_{op} depends on suction. Figure 6 shows the increase of E_{0p} with suction and therefore with the effective stress.

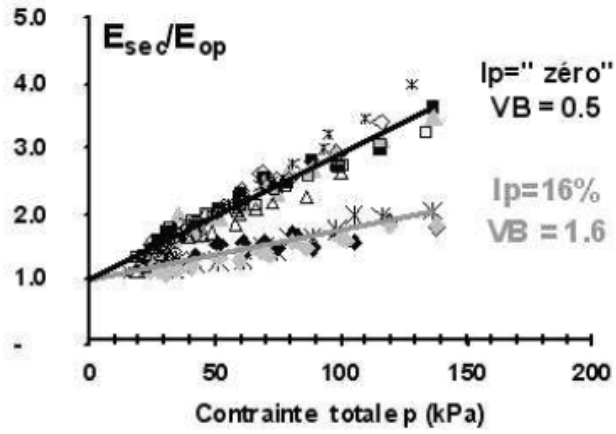

Figure 5: Normalization of the secant modulus as a function of the total mean stress p for plasticity indexes 0% and 16% and 10% of fines.

$$\frac{E_{\sec}}{E_{0p}} = 1 + 0.02 p_a \left(\frac{p}{p_a} \right) \quad \text{IP=0} \tag{2}$$

$$\frac{E_{\sec}}{E_{0p}} = 1 + 0.008 p_a \left(\frac{p}{p_a} \right) \quad \text{IP=16\%} \tag{3}$$

Where p_a is the atmospheric pressure.

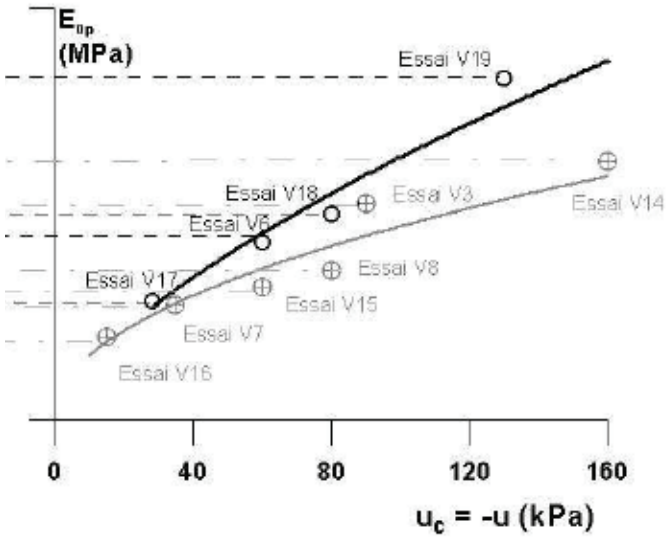

Figure 6: Relationship between the modulus E_{0p} and the suction for 10% of fines and IP=0 and IP=16%.

Figure 7 shows the normalized modulus E_{sec}/E_{op} in the plane (E_{sec}/E_{op}−p) for materials having 20% of fines and different plasticity indexes (5% and 12%). Also in this case, the slope of the lines increases as the plasticity index decreases but the variation is less significant than for the case of 10% of fines and plasticity indexes of 0% and 16%. Equations 4 and 5

describe the variation of modulus for the different plasticity indexes. Figure 8 shows the modulus E_{0p} related to suction for the two different plasticity indexes.

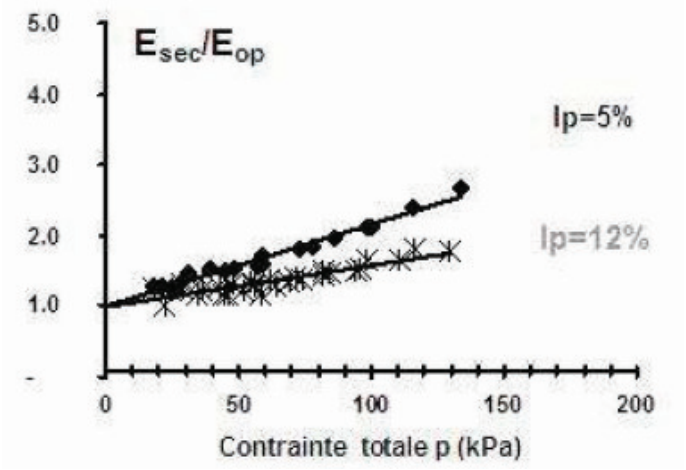

Figure 7: Normalization of the secant modulus as a function of the total mean stress p for a plasticity index of 5% and 12% and 20% of fines.

$$\frac{E_{\sec}}{E_{0p}} = 1 + 0.012 p_a \left(\frac{p}{p_a} \right) \quad \text{IP=5\%} \tag{4}$$

$$\frac{E_{\sec}}{E_{0p}} = 1 + 0.006 p_a \left(\frac{p}{p_a} \right) \quad \text{IP=12\%} \tag{5}$$

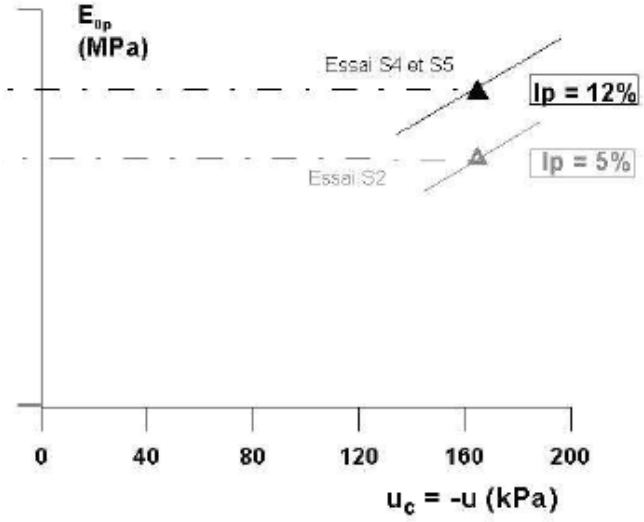

Figure 8: Relationship between the modulus E_{0p} and the suction for 20% of fines and IP=5% and IP=12%.

In the case of 30% of fines, we found that the plasticity index has a less significant role in the normalized plane that in the cases with smaller fine contents. In fact, Figure 9 shows that the slope of the lines in the plane (E_{sec}/E_{op}–p) is the same for the different plasticity indexes. Moreover, the modulus E_{0p} has a clear relationship with the suction (Figure 10).

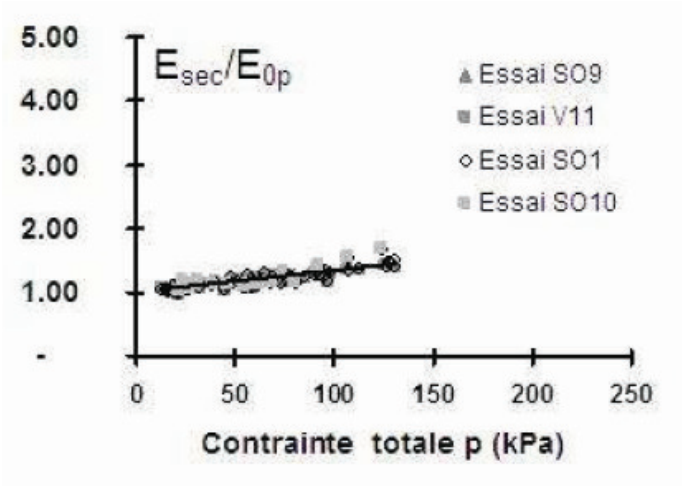

Figure 9: Normalization of the secant modulus as a function of the total mean stress p for 30% of fines and different plasticity indexes.

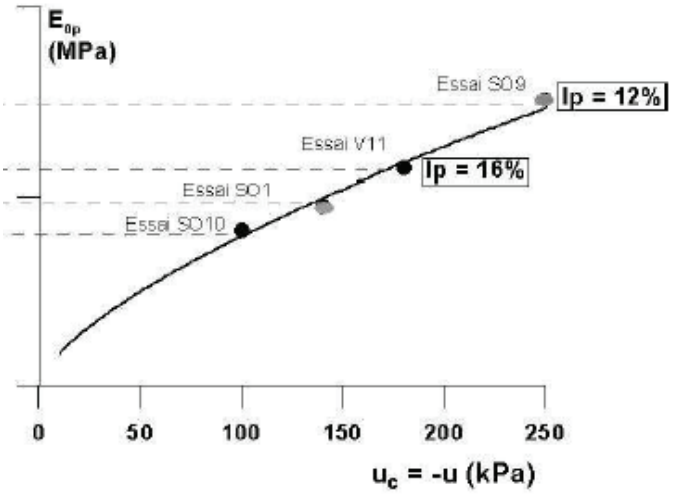

Figure 10: Relationship between the modulus E_{0p} and the suction for 30% of fines.

4 INTERPRETATION OF THE RESULTS USING EFFECTIVE STRESSES

Different expressions have been proposed to calculate the effective stress in an unsaturated medium. In the case of high negative pore water pressures and low degrees of saturation, the approach developed at the Ecole Centrale Paris is based on a micromechanical model composed of regular arrangements of non-deformable balls of the same diameter d (Fleureau et al. 2003).

The increase in negative pore water pressure due to the reduction of the degree of saturation leads to an increase in the intergranular forces, which increases the moduli and the shear strength of the soil. For a regular arrangement of spheres, an elementary calculation based on Laplace's law results in the following expression of the capillary stress p'_u that represents the contribution of the negative pore water pressure to the cohesion of the material. The capillary stress is a function of suction and of the diameter d. In the case of a real grain size distribution, the parameter d must be determined.

The expression to pass from total stresses to effective stresses is therefore:

$$\sigma_V^{'} = \sigma_V + p_u^{'} \qquad (6)$$

To compare the results of the tests carried out at different void ratios, it is necessary to normalize the moduli to the same value of void ratio. The relation of Iwasaki et al. (1978) was used to bring the moduli back to a void ratio of 0.33:

$$E_{(e=0.33)} = E_e \frac{f(e=0.33)}{f(e)} \quad f(e) = \frac{(1.93-e)^2}{1+e} \qquad (7)$$

For the Colombian materials, a simplified effective stress law has been used. This relationship was the Terzaghi law using the measured negative pore pressure. Figure 11 shows all the results of moduli obtained for the Vista Hermosa material in function of the effective isotropic stress. All the results can be described by a power equation.

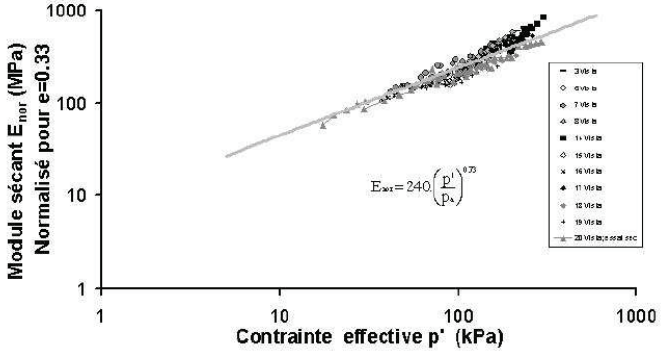

Figure 11: E_{sec} as a function of the isotropic effective stress for all the mixtures with Vista Hermosa Material.

What is more, all the results concerning Colombian materials can be considered in the same effective stress plane. In this case all the results can be described by a unique equation with limited scatter along the regression line (figure 12).

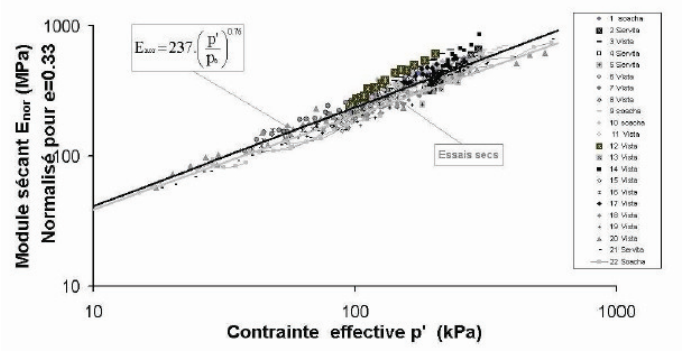

Figure 12: E_{sec} as a function of the isotropic effective stress for all the mixtures with Colombian materials.

5 CONCLUSIONS

The precision triaxial tests performed on three road unbound granular materials highlight the non linear behavior of these materials. The effect of the water content, plasticity index and fines content on the secant modulus is important. The interpretation of the results in terms of effective stresses based on suction measurements shows that it is possible to take into account the effect of water content on the reversible parameters. The role of the grain size distribution and crushability are directly related to the changes in suction.

These results allow to generalize the constitutive laws developed for dry untreated unbound granular materials to larger conditions of water content, representative of the real conditions in pavements.

6 REFERENCES

Balay, J., Gomes Correia, A., Jouve, P., Hornych, P. & Paute, J. 1998 Etude expérimentale et modélisation du comportement mécanique des graves nos traitées et des sols support de chaussées, Bull. Ponts & Ch., 216 : 3-18.

Biarez, J., Fleureau, J.M. & Kheirbek-Saoud, S., 1991. Validité de s'=s - uw dans un sol compacté, 10th E.C.S.M.F.E., Firenze, Vol. 1: 15-18.

Brull A. 1980. Caractéristiques mécaniques des sols de fondation de chaussées en fonction de leur état d'humidité et de compacité, Coll. Int. Compactage, Presses Ponts & Chaussées, Paris, Vol. 1: 113-118.

Coronado O., Caicedo B., Fleureau J.-M. & Gomes Correia A. 2004. Influence de la succion sur les propriétés d'un matériau granulaire routier, Compte-rendus du 57ème Congrès Canadien de Géotechnique « GeoQuébec2004 », Québec, Canada, 24-28 Octobre 2004.

Coussy, O. & Dangla, P. 2002. Approche énergétique du comportement des sols non saturés , in Mécanique des sols non saturés, Hermès, Paris : 137-174.

Goto, S., Tatsuoka, F., Shibuya, S., Kim Y.-S. & Sato, T. 1991. A simple gauge for local small strain measurements in the laboratory, Soils and Foundations, 31, 1 : 169-180.

Fleureau, J.-M., Hadiwardoyo, S. & Gomes Correia, A 2003. Generalised effective stress analysis of strength and small strains behaviour of a silty sand, from dry to saturated state, Soils and Foundations, 43, 4 : 21-33.

Iwasaki, T., Tatsuoka, F. and Takagi, Y. 1978. Shear Moduli of Sands under Cyclic Torsional Shear Loading, Soils and Foundations, 18, 1: 39-50.

Kheirbek-Saoud, S. 1994. PhD Thesis, Ecole Centrale Paris

Lekarp F., Isacson U., Dawson A. 2000. State of the art I: Resilient response of unbound aggregates. Journal of transportation engineering, February 2000.

Picornell, M. & Nazarian, S. 1998. Effects of soil suction on the low-strain shear modulus of soils, 2nd Int. Conf. on Unsat. Soils, Beijing, 2: 102-107.

Taibi, S. 1994. PhD Thesis, Ecole Centrale Paris.

Wu, S., Gray, D.H. & Richart, F.E. 1989. Capillary effects on dynamic modulus of sands and silts, Geot. Eng. Div. J., ASCE, 110 (9): 1188-1203.